Title: Early life sleep disruption alters glutamate and dendritic spines in prefrontal cortex and impairs cognitive flexibility in prairie voles

Authors: Carolyn E. Jones, [1,2], Alex Q. Chau[1], Randall J. Olson[1,2], Cynthia Moore, Peyton T. Wickham[1], Niyati Puranik[1], Marina Guizzetti,[1,2] Hung Cao,[3] Charles K. Meshul,[1,2] Miranda M. Lim,[1,2]*

Affiliations:
1. VA Portland Healthcare System, Portland, OR, USA
2. Oregon Health & Science University, Portland, OR, USA
3. University of California, Irvine

*Correspondence should be addressed to:
Miranda M. Lim, MD, PhD
3710 SW US Veterans Hospital Road
Mailcode P3-RD42
Portland, OR. 97239
L M I R @ O H S U . E D U

Keywords
Development, extinction, autism

Author Contributions
C.E.J. and M.M.L. designed experiments. C.E.J. and R.J.O. conducted and scored behavioral tests. P.T.W. and C.E.J. conducted Rapid Golgi staining and prepared brain tissue for analysis. A.Q.C. imaged dendritic spines with input from M.G.. N.P., C.M., and C.K.M. imaged and processed EM data. A.Q.C. and R.J.O. quantified spines. C.E.J., R.J.O., M.M.L., C.K.M., A.Q.C, and H.C. interpreted data. C.E.J., M.M.L, R.J.O, and P.T.W. wrote the manuscript with approval from all authors.

Acknowledgements
Mara E. Kaiser and Natasha Avalon Gardner for assistance with Golgi staining and brain sectioning, Elizabeth A.D. Hammock for initial discussion regarding experimental design, Calla Goeke for assistance with light microscopy.

Funding: NSF #1926818 to HC and MML, Portland VA Research Foundation to MML, NIH NHLBI 5T32HL083808-10 to CEJ, VA Merit Review #I01BX001643 to CKM, R01AA022948 and I01BX001819 to MG, Collins Foundation Grant to MML, Brain and Behavior Foundation NARSAD to MML.

Abstract

Early life experiences are crucial for proper organization of excitatory synapses within the brain, with outsized effects on late-maturing, experience-dependent regions such as the medial prefrontal cortex (mPFC). Previous work in our lab showed that early life sleep disruption (ELSD) from postnatal days 14-21 in the highly social prairie vole results in long lasting impairments in social behavior. Here, we further hypothesized that ELSD alters glutamatergic synapses in mPFC, thereby affecting cognitive flexibility, an mPFC-dependent behavior. ELSD caused impaired cued fear extinction (indicating cognitive inflexibility), increased dendritic spine density, and decreased glutamate immunogold-labeling in vesicular glutamate transporter 1 (vGLUT1)-labeled presynaptic nerve terminals within mPFC. Our results have profound implications for neurodevelopmental disorders in humans such as autism spectrum disorder that also show poor sleep, impaired social behavior, cognitive inflexibility, as well as altered dendritic spine density and glutamate changes in mPFC, and imply that poor sleep may cause these changes.

MAIN TEXT

Introduction

Early in development, neural synapses undergo morphological and functional changes necessary for the expression of species-typical adult behavior. Considerable research suggests synaptic reorganization, including synapse formation, growth, and pruning, is differentially shaped by rapid eye movement (REM), non-REM (NREM), and awake states [1-3]. These processes are especially sensitive to perturbations in sleep early in development [4-6] when sleep amounts are highest [7]. In both humans and rodents, REM sleep time is especially high early in life comprising nearly 50% of all sleep. An age-related reduction in REM, typically occurring at ~2 years old in humans [7] and approximately 14-21 days old in rodents [8-10] may indicate a shift in the function of REM sleep from synaptic reorganization to neural repair that is conserved across species [11].

Glutamate is differentially released within different brain regions across the various sleep-wake states [12, 13], and also plays a critical role in the stabilization and maturation of excitatory synapses [14]. Excitatory neurotransmission in mammals is driven, in part, by presynaptic vesicular glutamate release. This release is regulated by vesicular glutamate transporters, primarily vGLUT1 and vGLUT2, which are expressed in non-overlapping populations of presynaptic nerve terminals in the mammalian cortex [15]. These terminals primarily make an asymmetrical synaptic contact onto dendritic spines, and spine morphology and density can inform how excitatory signals are processed [16, 17]. Accordingly, neurodevelopmental disorders commonly feature abnormalities in glutamate neurotransmission and related glutamatergic structures (e.g., dendritic spines, vGLUT1/2, and other excitatory synaptic markers)[18-20] along with altered sleep patterns compared to typically developing children [21].

Higher order social learning, executive function, and cognitive flexibility in humans and rodents depends on the functioning of the prefrontal cortex (PFC) (see [22, 23] for review).

Subregions of the rodent PFC govern tasks requiring cognitive flexibility and rule change, including the extinction of emotionally salient associations [24-28] such as in cued fear. In both humans and rodents, the PFC is a late-maturing region with an extended sensitive period to experiences and environmental insults. Accordingly, the PFC is often affected in neurodevelopmental disorders such as autism spectrum disorder (ASD), leading to characteristic impairments in social behavior and cognitive flexibility [29, 30].

Our recent research using the highly social prairie vole has shown that early life sleep disruption (ELSD), using a method that substantially reduces REM sleep but also increases wakefulness and fragments NREM sleep [31-33], results in long-term impairments in social behavior [31]. Notably, using this method, there are no changes in measures of stress such as body mass, serum corticosterone, parental care, or anxiety-like behavior [31, 32, 34]. Here, we hypothesized that ELSD specifically affects glutamatergic neurotransmission in the late-maturing mPFC. In order to test this hypothesis, we examined effects of ELSD on 1) cognitive flexibility through cued fear extinction, a mPFC-dependent behavior, and 2) glutamatergic synaptic structure within the mPFC using a combination of light microscopic quantification of dendritic spines and ultrastructural immunohistochemical analysis using electron microscopy.

Results

In all experiments, prairie voles underwent either an Early Life Sleep Disruption (ELSD) paradigm or Control conditions continuously from postnatal days (P) 14 -21 [31, 34]. Male and female prairie voles were weaned on P21 and left undisturbed until adulthood (range: P70-110, see methods for details), at which point they were tested in one of three experiments: 1) behavioral testing for cued fear conditioning and extinction, 2) dendritic spine quantification and morphology using Rapid Golgi staining of pyramidal neurons in both superficial and deep layers of the mPFC including both infra- and pre-limbic cortices, or 3) electron microscopy of vGlut1 and vGlut2 labeled synapses.

ELSD impairs extinction acquisition after cued fear conditioning

In Experiment 1, cognitive flexibility was measured by first exposing voles to cued fear conditioning (tone cue paired with a mild footshock) followed by two days of extinction (19 non-reinforced cue presentations per session; **Fig 1a** for experimental timeline). Cognitive flexibility was inferred when voles showed decreased freezing behavior, an expression of fear, during the extinction sessions after first learning to display a fear response to the cue. Males (ELSD n= 14; Control n=10) and females (ELSD n=8; Control n=10) are combined for visual representation (**Fig 1**).

On the first extinction day (**Fig 1b**), there was a significant within subjects effect of conditioned stimulus (CS) number on freezing levels (repeated measures ANOVA, within subjects factor CS number: $F(18,684) = 21.509$, $p<0.0001$) as well as a significant interaction between freezing over the first extinction period and early life sleep group (repeated measures ANOVA, CS number x sleep group interaction: $F(18,684)=2.573$, $p=0.007$). During the second day of extinction (**Fig 1c**) there was also a significant reduction of freezing over CS number (repeated measures ANOVA, within subjects effect of CS number: $F(18,630)=13.583$, $p<0.0001$). This rate of reduction was no longer influenced by the ELSD group (repeated measures ANOVA, CS number x sleep group interaction: $F(18,630)=0.906$, $p=0.528$), nor was it influenced by sex (repeated measures ANOVA, CS number x sex interaction: $F(18,630)=0.923$, $p=0.512$). Overall, ELSD voles froze more than Controls during both extinction sessions (Extinction 1: effect of sleep group: $F(1,38)=5.651$, $p=0.023$; Extinction 2: effect of sleep group: $F(1,35)=24.985$, $p<0.0001$) and there were no significant effects of sex (Extinction 1: effect of sex: $F(1,38)=0.002$, $p=0.966$; Extinction 2: effect of sex: $F(1,35)=2.845$, $p=0.101$) or interactions (Extinction 1: sleep group x sex interaction $F(1,38)=0.008$, $p=0.928$; Extinction 2: sleep group x sex interaction: $F(1,35)=2.448$, $p=0.127$).

A subset of animals (n=18) were tested 24 hours later for long-term extinction retention with three CS presentations (**Fig 1d**). ELSD voles froze significantly more than Controls over the three cues (repeated measures ANOVA, between group effect of sleep group: $F(1,14)=22.448$, $p<0.001$) which was driven by increased freezing in the males (repeated measures ANOVA, sleep group x sex interaction: $F(1,14)=5.077$, $p=0.041$). There was not a main effect of sex on freezing during the long-term memory test (repeated measures ANOVA, between group effect of sex: $F(1,14)=1.175$, $p=0.297$).

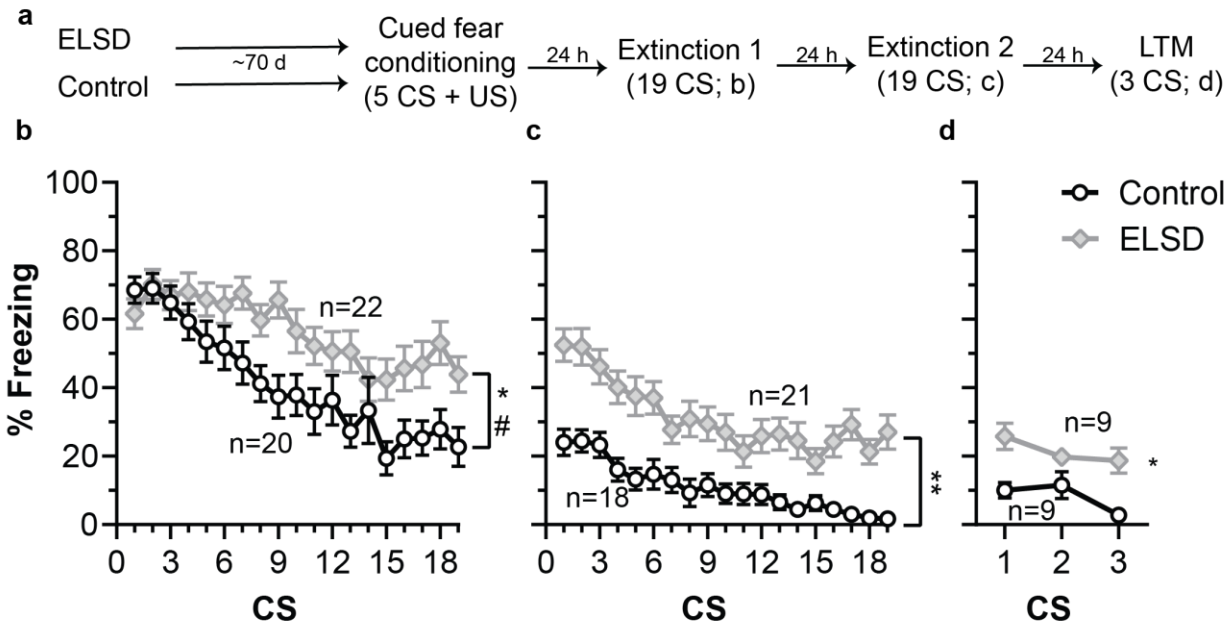

Figure 1: Freezing during extinction and long-term memory sessions. a) Timeline depicting order of tests in Experiment 1. b, c) ELSD voles extinguished slower and less completely than Controls during both days of extinction despite similar levels of freezing at the beginning of extinction 1 (c). d) Long-term memory tests of extinction indicate that both groups retain their levels of extinction but ELSD voles froze more than Controls. Data are mean +/- SEM. Asterisks indicate significant between group effects. *$p<0.05$, **$p<0.01$. # indicates significant group x CS number interaction $p<0.05$. US = unconditioned stimulus; CS = conditioned stimulus

ELSD increases spine density in PL Layers 2/3 – Rapid Golgi

Based on the fear extinction behavior, our *a priori* hypothesis was that the mPFC would show changes in dendritic spine density after ELSD, as assessed by Rapid Golgi staining. Within the rodent PFC, tasks requiring cognitive flexibility and rule change depend on functioning of the medial subregions, with opposing roles of the more dorsally located prelimbic region (PL) and the more ventrally located infralimbic region (IL) in activation and inhibition of fear responses, respectively[28]. Based on this literature, we further hypothesized that PL and IL would show unique responses to ELSD due to their opposing roles in extinction learning. Separate ANOVAs were used to analyze data for Layers 2/3 and Layer 5 and alpha values were Bonferroni corrected to account for multiple comparisons (with correction, $p < 0.025$ is needed to reject the null hypothesis).

In Layers 2/3 of PL, there were significantly more spines per µm in ELSD animals (n=7 males; m=6 females) compared to Controls (n=8 males; n=4 females) (ANOVA, main effect of sleep group: $F(1,21)=24.614$, $p<0.0001$) and no significant effect of sex (ANOVA, main effect of sex: $F(1,21)=2.087$, $p=0.163$; sleep group x sex interaction: $F(1,21)=1.127$, $p=0.301$) (**Fig 2a, left panel**). In Layer 2/3 of IL, ELSD did not affect spine density (ANOVA, main effect of sleep group; $F(1,15)=0.858$, $p=0.369$) but there was a trend towards a main effect of sex, with increased spine density in female voles (ANOVA, main effect of sex: $F(1,15)=4.323$, $p=0.055$; group x sex interaction; $F(1,15)=4.734$, $p=0.046$) that did not meet significance requirements with post-hoc corrections for multiple cortical layers (**Fig 2a, right panel**) (n=5 Control males; n=4 Control females; n=5 ELSD males; n=5 ELSD females). There were no significant differences in spine density in Layer 5 of PL (ANOVA, main effect of sleep group: $F(1,12)=0.231$, $p=0.639$, main effect of sex; $F(1,12)=3.378$, $p=0.091$; group x sex interaction: $F(1,12)=0.147$, $p=0.708$) (**Fig 2a, right panel**) (n=6 Control males; n=2 Control females; n=5 ELSD males; n=5 ELSD females), or IL cortices (ANOVA, main effect of sleep group: $F(1,12)=0.231$, $p=0.639$, main effect of sex; $F(1,12)=3.378$, $p=0.091$; group x sex interaction:

F(1,12)=0.147, *p*=0.708) (**Fig 2a, right panel**) (n=2 Control males, n=4 Control females; n=5 ELSD males; n=5 ELSD females).

ELSD causes thinner spines in PL Layers 2/3 – Rapid Golgi

Spine morphology was quantified as an indicator of maturity using the average length:width ratio (LWR) for spines in each segment and analyzed in an identical manner as spine density. In Layer 2/3 of PL, voles that underwent ELSD from P14-21 had higher LWR compared to controls indicative of longer and thinner spine morphology (**Fig 2b, left panel**) (ANOVA, main effect of group: *F*(1,21)=20.520, *p*=0.0002) and females had higher LWR compared to males (ANOVA, main effect of sex: *F*(1,21)=18.564, *p*=0.0003), but the interaction did not reach significance (ANOVA, sleep group x sex interaction; *F*(1,21)=3.862, *p*=0.063). LWR were also higher after ELSD in Layer 2/3 of IL (**Fig 2b, right panel**) (ANOVA, main effect of sleep group: *F*(1,15)=7.379, *p*=0.016) and the effect of sex did not reach significance (ANOVA, main effect of sex: *F*(1,15)=3.254, *p*=0.091; group x sex interaction; *F*(1,15)=1.872, *p*=0.191). There was no effect of ELSD on LWR in Layer 5 of PL (**Fig 2b, left panel**) (ANOVA, main effect of sleep group: *F*(1,14)=0.275, *p*=0.608) and no effect of sex (ANOVA, main effect of sex: *F*(1,14)=0.628, *p*=0.441; group x sex interaction; F(1,14)=1.970, *p*=0.182), nor in Layer 5 of IL (**Fig 2b, right panel**) (ANOVA, main effect of group: *F*(1,12)=3.184, *p*=0.100) nor an effect of sex (ANOVA, main effect of sex: *F*(1,15)=1.576, *p*=0.233; group x sex interaction: *F*(1,15)=2.231, *p*=0.161).

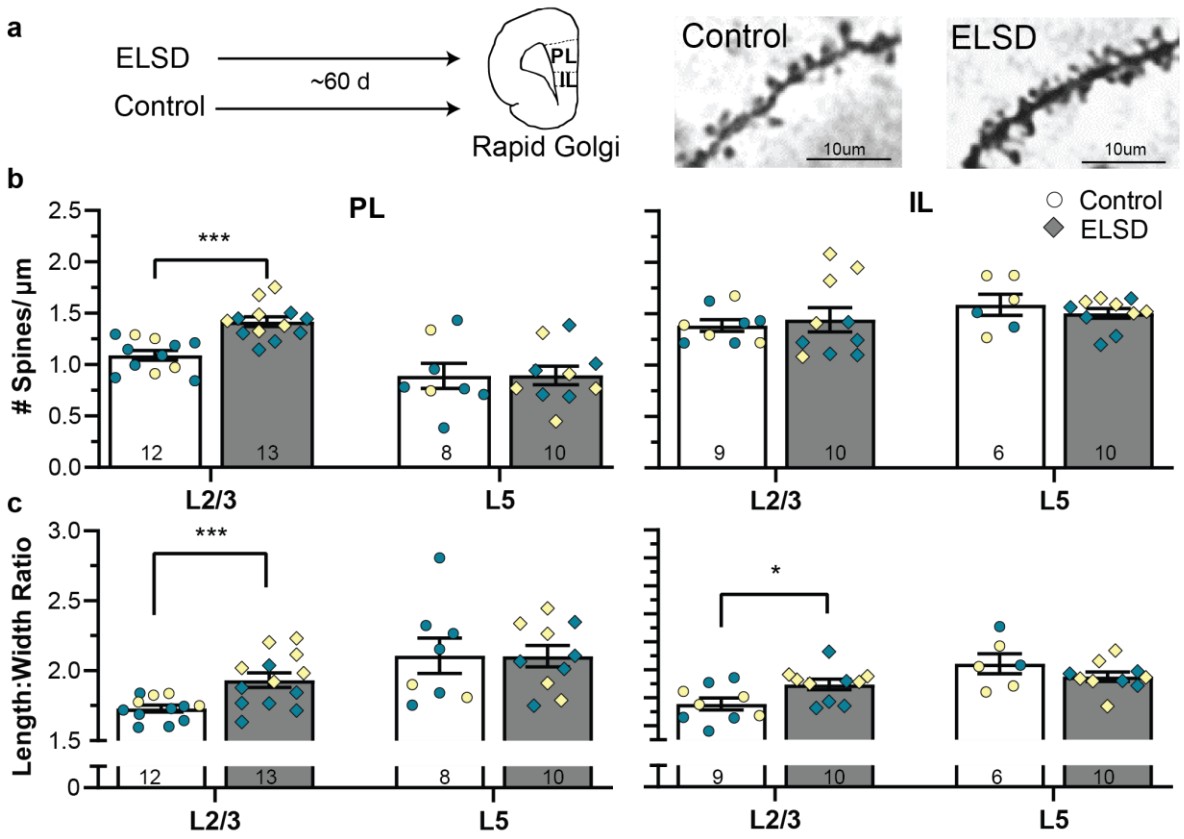

Figure 2: Dendritic spine density and morphology quantified with Rapid Golgi staining in prelimbic (PL) and infralimbic (IL) prefrontal cortex. a) Experimental timeline and representative image (40x) of Rapid Golgi-stained dendritic spines from Layer 2/3 PL after Control or ELSD conditions. b) Number of spines per µm in PL and IL cortices. ELSD from P14-P21 (grey bars) resulted in an increase in dendritic spine density in Layers 2/3 of PL (left panel) compared to Controls (white bars). There was no significant difference in spine density in IL (right panel) c) Length:Width ratio (LWR) was increased in Layer 2/3 in both PL and IL after ELSD compared to Control conditions. Higher LWR indicates longer and thinner spines. Number underneath bars indicates the number of animals used for analysis. Bar height is mean, error bars +/- SEM, individual data points colored by sex (female voles = yellow, male voles = teal). *p<0.025; ***p<0.0005

ELSD decreases the density of glutamate immuno-gold labeling and size of vGLUT1-labeled presynaptic nerve terminals in PL Layer 2/3 – Electron Microscopy

Given our finding of increased spine density and changes in spine morphology (increased LWR) within PL Layers 2/3 after ELSD, we next focused specifically upon examination of ultrastructural changes within glutamatergic synapses of Layers 2/3 of PL. Sections were double-labeled with either glutamate-immunogold + vGLUT1 or glutamate-immunogold + vGLUT2. vGLUT1-labeled presynaptic nerve terminals are presumed to originate from cortico-cortical synaptic inputs into the mPFC, whereas vGLUT2-labeled presynaptic nerve terminals are presumed to originate from thalamic inputs into the mPFC [35, 36].

In vGLUT1-labeled presynaptic nerve terminals, glutamate density (number glutamate immuno-gold particles/μm^2) was lower in ELSD voles (n=8; 5 male and 3 female) compared to Controls (n=6; 3 males and 3 females) (independent samples t-test, two tailed: $t(12)=3.149$; $p=0.008$). Glutamate density was not affected by early life sleep group (Control n=5 (3 males, 2 females); ELSD n=7 (3 males, 4 females) in vGLUT2-labeled terminals (independent samples t-test, two-tailed: $t(12)=0.838$, $p=0.421$;) (**Fig 3b**).

Consistent with our results from Golgi-stained tissue showing increased LWR of dendritic spines, both vGLUT1-labeled presynaptic nerve terminal area and its corresponding dendritic spine area were significantly lower in ELSD voles (n=7: 4 males, 3 females) than Controls (spines: n=6: 3 males, 3 females; pre-synaptic area: n=9: 6 males, 3 females) (independent samples t-test, two tailed: spines $t(11)=2.605$; $p=0.024$; pre-synaptic area $t(14)=4.259$, $p=0.001$) (**Fig 3c, d**). There was no difference in the average presynaptic terminal area of vGLUT2-labeled terminals (independent samples t-test, two tailed: $t(11)=1.793$, $p=0.100$) nor their corresponding spine areas (independent samples t-test, two tailed: $t(11)=.369$, $p=0.719$) between ELSD (spines: n=7, 4 males, 3 females; pre-synaptic area: n=7, 3 males, 4 females) and Controls (n=6, 4 males, 2 females).

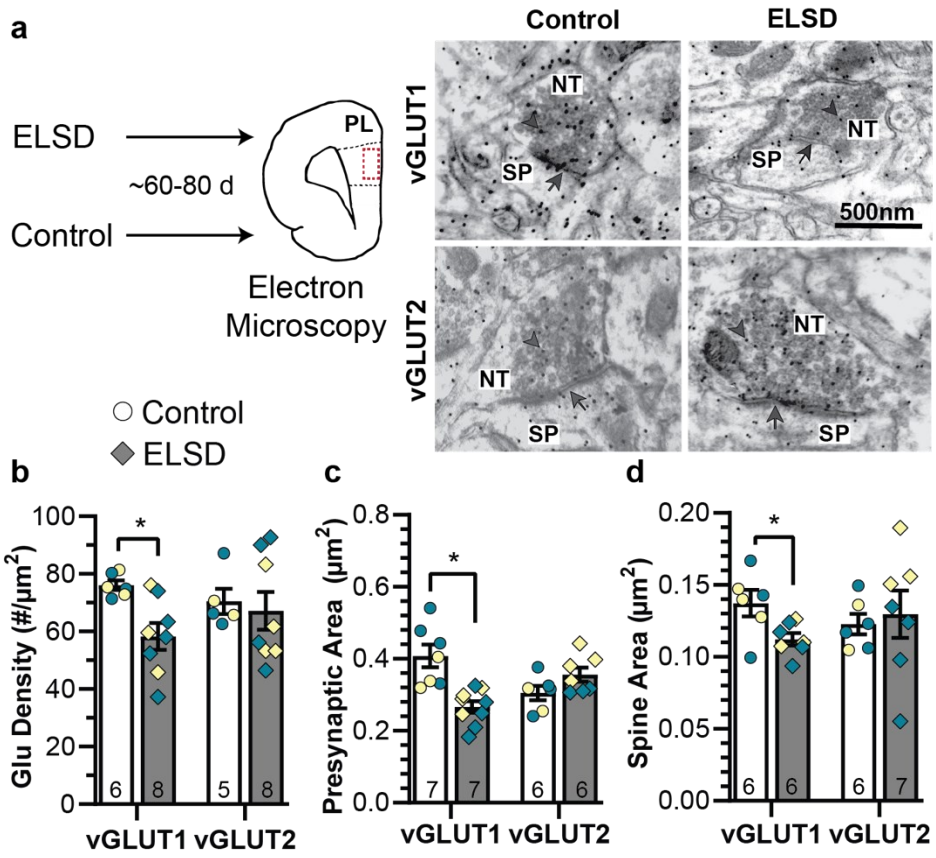

Figure 3 – Ultrastructural analysis of vGLUT1- and vGLUT2-labeled terminals and associated spines in Layers 2/3 of PL. a) Representative image of DAB-labeled nerve terminal making an asymmetrical synaptic contact with an underlying spine in adult voles that underwent Control or ELSD early life conditions (darkened material inside the terminal is DAB-diaminobenzidene, showing the localization of the antibody against vGLUT1 or vGLUT2). Arrowhead inside nerve terminal is pointing to 12nm glutamate gold particle, showing the localization of the glutamate antibody. Arrow indicates an asymmetrical synaptic contact. b) Average density of glutamate gold particles in vGLUT1-labeled terminals was decreased after ELSD compared to Controls but not in vGLTU2-labeled terminals. c) ELSD decreased average presynaptic nerve terminal area compared to controls in terminals labeled with vGLUT1, but not vGLUT2. d) ELSD decreased average area of spines in the corresponding postsynaptic targets of vGLUT1-labeled terminals, but not vGLUT2, compared to Controls. Bar height is mean; Error bars are SEM; number at bottom of bars is n per group; *p<0.05; Individual data points represent average values per animal. Teal = males; yellow = females; NT = nerve terminal; SP = spine.

Discussion:

We have previously shown in the highly social prairie vole that early life sleep disruption (ELSD) during the third postnatal week of development, resulted in a profound impairment in social behavior later in life [37]. Here, we show that adult voles that underwent ELSD also showed significantly impaired extinction of cued fear, a behavior that is dependent on mPFC development [38] and could be attributed to impaired cognitive flexibility. Furthermore, adult voles subjected to ELSD showed increased dendritic spine density and spine immaturity, as well as decreased glutamate labeling within vGLUT1+ nerve terminals, both indicative of altered glutamatergic neurotransmission within the prelimbic (PL) region of the mPFC. Our experimental results mirror human neurodevelopmental disorders including autism spectrum disorder that also show poor sleep, impaired social behavior, cognitive inflexibility, as well as altered dendritic spine density and glutamate changes in mPFC. Taken together, these results have profound implications about the directionality and potential mechanisms underlying the relationship between early life sleep, neural plasticity, and behavioral development.

ELSD impairs cognitive flexibility

We found that ELSD voles did not extinguish a cued fear association to the same level as Controls, indicating impaired cognitive flexibility. In humans with ASD, cognitive and behavioral rigidity are measured in laboratory settings through deficits in reversal learning [39, 40] and extinction [41]. Accordingly, animal models of ASD also show similar impairments in reversal learning (e.g. *Oxtr*-/- mouse line [42]) and fear extinction (e.g. VPA exposed rats [43, 44]), supporting the use of this behavioral test as a measure of cognitive flexibility.

Furthermore, we found that ELSD voles showed higher levels of freezing behavior during extinction and long-term memory tests, indicative of increased emotional responding during and after extinction. Although ELSD voles did not extinguish as completely as Controls, there was no impairment in recalling the extinction memory that was formed after 24 hours, a

behavior that relies on the IL subregion of the mPFC [24, 45] and was therefore not the focus of these studies. However, ELSD and Control voles froze at similar levels during the early cues of extinction suggesting that the acquisition and long-term (24 hrs) retention of an auditory cued fear association is not affected by ELSD. Extinction of cued fear is a mPFC-dependent task, a brain region of particular relevance to ELSD given its experience-dependent maturation that occurs throughout the early postnatal period. Cued fear extinction requires reversal and suppression of previously learned fear responses. At the neural level, cued fear extinction recruits a circuit involving the amygdala, hippocampus, and both the PL and IL subregions of mPFC. These mPFC regions are well documented in the literature for their opposing responses to fear learning and extinction: with the PL activating the fear response and the IL inhibiting fear responding via direct and indirect connections with the amygdala [45, 46].

Our results suggest that ELSD may affect behavioral response selection when faced with an emotionally salient challenge, including a cue that previously signaled a footshock, or similarly, partner preference behavior [31].

ELSD increases immature spines in PL Layers 2/3

Given the dependence of extinction behavior on both PL and IL subregions of the mPFC, we next examined the morphology of dendritic spines on pyramidal neurons in both the PL and IL of adult ELSD or Control voles. We found that spine density in PL (but not IL) was increased in ELSD voles compared to Controls, and that this effect was specific to mPFC Layers 2/3. Furthermore, we found that spine length to width ratio was also increased in Layer 2/3 in ELSD voles compared to Controls, indicating longer/thinner spines and a potential shift towards immaturity [47]. These effects were not present in Layer 5.

In the rodent mPFC, PL is positioned to integrate both limbic and sensory information from the neocortex. While the rodent PL and IL both receive afferent projections from primarily limbic regions and the midline thalamus [48-51], the main anatomical difference is the origin of

their cortical inputs. Afferents to PL come from other areas of PFC, whereas afferents to IL come from PL and, more strongly, hippocampal CA1. Thus, PL contains strong cortico-cortical connections with other frontal regions responsible for integrating sensory, limbic, and timing information [49]. The specificity of effects of ELSD on dendritic spine density within PL (and not IL) may indicate a developmental vulnerability for neocortical inputs.

The layers of the mammalian cortex reveal a topographic organization that informs function; pyramidal neurons in the superficial cortical layers have characteristic connectivity with other cortical regions. Within the rodent mPFC, thalamic afferents are most prominent in deeper layers (e.g., Layers 4 and 5), compared to more superficial layers (e.g. Layers 2/3), where afferents tend to be from adjacent PFC and other cortical regions [49]. The fact that we observed changes in Layers 2/3 and not Layer 5 suggests that the cortical, rather than thalamic, afferents to mPFC are more sensitive to ELSD during this particular developmental window of P14-21.

Spine development in the human PFC also occurs postnatally during an extended developmental window within the superficial cortical layers (e.g. Layers 2/3) [52, 53]. Postmortem analysis of brains from humans with ASD also report increased spine density on apical dendrites of pyramidal neurons compared to age matched, typically developing Controls, an effect most pronounced in Layer 2 [18]. Although impossible to compare rodent and human development at all levels, in terms of cortical maturation, P12-13 of a rodent approximates the period corresponding to full term birth in a human infant [54]. Human studies thus support our hypothesis that the PFC may be especially sensitive to environmental insults that occur after birth, such as sleep disruption.

ELSD decreases glutamate density, as well as nerve terminal and spine areas, within vGLUT1+ structures

Given our finding of increased spine density and spine immaturity within PL Layers 2/3 after ELSD, we next examined ultrastructural changes within glutamatergic synapses within Layers 2/3 of PL. We examined features of both pre- and post-synaptic contacts of terminals labeled with either one of two vesicular glutamate transporter types: vGLUT1 and vGLUT2. After ELSD, the density of glutamate immunogold particles, following exposure of the sectioned tissue to an antibody against glutamate, within vGLUT1-labeled terminals was significantly decreased. This effect was specific to vGLUT1, as it was not observed within vGLUT2-labeled terminals. Furthermore, ELSD decreased both presynaptic nerve terminal and post-synaptic spine area in vGLUT1-, but not vGLUT2-labeled terminals. This is consistent with our earlier findings of increased spine density and thinner dendritic spines in Layers 2/3 mPFC. Combined, these data suggest that ELSD results in a fundamental shift to an increase in smaller and more immature spines in ELSD animals [55].

The specificity of our findings to only vGLUT1-labeled terminals may have several implications. First, it could suggest that cortico-cortical connections (vGLUT1), rather than thalamocortical connections (vGLUT2) may be preferentially affected by ELSD. This is consistent with our previous findings using Rapid Golgi staining showing a differential effect of ELSD in Layer 2/3, but not Layer 5. Second, vGLUT1 expression is crucially upregulated in the rodent cortex during the third postnatal week of development, corresponding to the start of ELSD, whereas cortical vGLUT2 is most abundant in the first two weeks of postnatal life [56-58]. Thus, it makes sense that vGLUT1 inputs may be preferentially affected by ELSD during the third postnatal week. Finally, as cortico-cortical connections, especially long-range connections, are important for higher order integrative functions within cortical association areas, this may have implications for ELSD's long-term effects on processing, learning, and initiating behavioral responses to complex social cues.

Our finding that vGLUT1-labeled synapses (terminals and their associated spines) are smaller in area after ELSD is consistent with the possibility that the post-synaptic spines are

less mature. If vGLUT1-positive long-range cortico-cortical inputs to PL are preferentially impaired by ELSD, this could conceivably lead to a higher number of immature spines in PL, by virtue of less excitatory stimulation to these spines. Immature spines would be less functional with regard to neurotransmission, although follow-up electrophysiological experiments are warranted to confirm this hypothesis [59].

Potential mechanisms, limitations, and implications

Potential mechanisms explaining these findings could include one or both of the following possibilities: 1) increased wake during ELSD leads to increased glutamate in the brain [60] with long term effects on developmentally-sensitive glutamatergic structures [14], or 2) decreased REM or fragmented NREM sleep leads to decreased pruning of spines and impaired development of glutamatergic synapses [11].

There are several limitations to this study. One possible interpretation is that our effects could be due to the stress of ELSD. Although prior evidence suggests that changes to spine density on Layer 2/3 pyramidal neurons can occur due to stress or in response to corticosterone [61-63], we have found no difference in anxiety-like behaviors or serum levels of corticosterone in voles that undergo ELSD compared to controls [31]. Furthermore, most studies indicate spine loss in apical dendrites within Layers 2/3 of the mPFC [61, 64-66] where our results are most consistent with spine growth or lack of pruning of spines after ELSD.

A second limitation is the focus on the third postnatal week of development. While this period has been implicated in many developmental studies across species, including for sleep ontogeny [11], vGLUT1/2 expression [56], and dendritic spine development within PFC [see [67] for review], it is unclear whether this is a critical window or simply a sensitive period during development for effects of ELSD. Future work will examine ELSD at different developmental time points to answer this question.

Finally, a remaining question is how social behavior and cognitive flexibility, both hallmarks of ASD, integrate within the PFC not only in this vole model, but also in humans with ASD. It is possible individuals with impaired social function also have a similar degree of cognitive rigidity, and that a single circuit within the PFC underlies both complex behaviors [26-28, 45, 68-71]. Future studies would need to examine both sociality and cognition within the same individual for a more comprehensive understanding of their interaction, and extend studies beyond glutamate to include commonly co-released neuropeptides such as oxytocin [see [72]]. For example, in prairie voles, activation of oxytocin receptors in the prelimbic region are necessary for social bonding [73]. Additionally, direct activation of glutamatergic neurons that express oxytocin receptors in PL alter social behaviors in mice [74]. Interestingly, oxytocin receptor density peaks at P14 in the developing rodent cortex, with the densest distribution of receptors located in Layers 2/3 [75]. Thus, future work should also examine patterns of oxytocin receptor development in PL and its relationship to glutamate after ELSD.

Our work has strong parallels with ASD. Neuropathological studies in patients with ASD have shown increased spine density within the cortex [18]. Additionally, sleep problems are highly prevalent in patients with ASD, include decreased time in REM and fragmented sleep [21], an early life sleep pattern mirrored by our ELSD protocol. Although ASD is typically diagnosed around 3-5 years of age, behavioral and sleep deficits persist into adulthood. Emerging evidence suggests that sleep onset problems in the first year of life precede ASD diagnosis and are associated with altered neurodevelopment, consistent with our hypothesis that there is a causal role between early life sleep disruption and the later emergence of ASD [76, 77].

Conclusion

We have now shown, using the highly social prairie vole, that early life sleep disruption during the third postnatal week of development - a time period corresponding to the human first

year of life - results in long term impairments in social behavior [31], reduced cognitive flexibility, and altered glutamatergic synapse structures within the medial prefrontal cortex. Our results support the hypothesis that early life experiences directly shape brain structure and function, with particularly outsized effects on late-maturing, experience-dependent regions such as the prefrontal cortex. Because human neurodevelopmental disorders including autism spectrum disorder also show poor sleep, impaired social behavior, cognitive inflexibility, as well as altered dendritic spine density and glutamate changes, our results have profound implications about the directionality and potential mechanisms underlying the relationship between early life sleep, neural plasticity, and behavioral development.

Materials and Methods

Experimental Design

Three experiments were run in separate cohorts of animals to evaluate behavioral and glutamatergic features in the adult prairie vole medial prefrontal cortex (mPFC) after either early life sleep disruption (ELSD) or control conditions early in life. In Experiment 1, cognitive flexibility to an emotional stimulus was quantified with cued fear conditioning followed by cued extinction. In Experiment 2, apical dendritic spine morphology of pyramidal neurons was quantified using Rapid Golgi staining in the prelimbic (PL) and infralimbic (IL) regions of the mPFC. In Experiment 3, ultrastructural features including glutamate density and size of vesicular glutamate transporter 1 (vGLUT1) and vesicular glutamate transporter 2 (vGLUT2) labeled presynaptic terminals and corresponding post-synaptic spines were quantified with electron microscopy in Layer 2/3 of the prelimbic cortex. All experimental procedures were approved by the Institutional Animal Care and Use Committee at the Portland VA Medical Center and were conducted in accordance with guidelines set forth by the National Institutes of Health Guide for Care and Use of Laboratory Animals.

Subjects

Subjects were male and female adult prairie voles housed in clear polycarbonate cages (27 cm x 27 cm x 13 cm) in 14:10 light:dark cycle with lights on at 0700h. Subjects were bred at our colony at the Portland VA, sourced from 48 litters from 22 breeder pairs and reared by both parents. The prairie vole colony originated from a colony at Emory University derived from field-caught prairie voles in Illinois. Colony diversity was maintained through generous bi-annual donations from researchers across the United States, most recently Dr. Lisa McGraw at North Carolina State University in 2014, Dr. Karen Bales at UC Davis in 2015, Dr. Zoe Donaldson at CU Boulder in 2017, and Dr. Zuoxin Wang at FSU in 2019. Breeder pairs were checked each morning at lights on for the presence of pups and the day of pup discovery was designated as

postnatal day 1. Voles were weaned at P21 and socially housed with same sex littermates (2-4/cage). Female prairie voles were rehoused to a female-only colony room at this time, as they are male-induced ovulators, and are presumed to have been in anestrus for the duration of this study. Prairie voles had *ad libitum* access to water and a mixed diet of rabbit chow (LabDiet Hi-Fiber Rabbit), corn (Nutrena Cleaned Grains), and oats (Grainland Select Grains). Cotton nestlets and a wooden block or stick for chewing enrichment were added to each cage and replaced weekly.

ELSD paradigm

Prairie vole litters in their home cages were placed on a standard laboratory orbital shaker for one week, with both parents, from postnatal days 14-21 (ELSD group). The orbital shaker was programmed with an automatic timer to gently agitate the cage at continuous intervals at 110 RPM (10 seconds every 110 seconds; See [31]). Modifications to standard housing consisted of replacing water bottles with hydrogel to prevent leaking and cage cards were secured to prevent excessive auditory disturbance. The control group consisted of litters transferred to the same colony room containing the shakers from P14-P21 but were not physically sleep disrupted. Control cages had hydrogel added to cages but retained their water bottles as an additional source of hydration. We have previously found that this method of sleep disruption does not increase serum corticosterone levels in pups and does not alter parental care [31].

Experiment 1 –Cued fear conditioning and extinction

Adult prairie voles (P75-P90) that had undergone either ELSD (n=14 male; n=8 female) or control (n=8 male; n=10 female) early life sleep conditions underwent a four-day cued fear conditioning and extinction paradigm. Voles underwent cued fear conditioning followed by two days of extinction and finishing with one day of long-term memory tests for extinction retention. Each procedure was separated by 24 hours and conducted in the second half of the light cycle. Behavioral tests were conducted by the same experimenter each day (C.E.J.).

Apparatus and stimuli

All fear conditioning procedures took place in clear plexiglass chambers (40.8 cm x 14 cm x 18.4 cm) within black sound attenuating chambers fitted with fans, which provided background white noise at ~60 dB. Fear conditioning chambers were equipped with steel rod floors connected to a shock generator (Omnitech). Behavior was recorded with digital cameras (GoPro Hero5 Session) mounted inside each unit. Chambers were wiped with water and patted dry between each animal. The CS was a tone (3 kHz, 80 dB) 10 s in duration, and the US was a 0.7 mA foot-shock, 1 s in duration.

Behavioral testing procedures

Fear conditioning (day 1) – after a 6 minute habituation to the chamber each vole received 5 CS presentations (fixed inter-trial interval = 60 s), each co-terminating with the US. After fear conditioning, voles were immediately removed from the chambers and returned to their home cage. All cagemates were fear conditioned according to the same parameters and remained socially housed throughout the duration of the experiment.

Extinction 1 and 2 (days 2 and 3) – after a 6 minute habitation, each vole received 19 CS presentations in the absence of the US (fixed ITI = 60 s) in the same context as fear conditioning. Voles underwent two extinction sessions separated by 24 hours.

Long-term memory (day 4) – approximately half of the voles (n=9 Control and n=9 ELSD) underwent long-term memory tests on day 4 to test for extinction retention. Long-term memory tests consisted of 3 CS presentations in the absence of the US (fixed ITI = 60 s). The other half were not tested on this day due to equipment failure.

Scoring and analysis

Videos were watched by a trained experimenter (C.E.J.) blind to both sex and early life sleep condition and total time freezing was scored with a digital stopwatch for the duration of each CS. Freezing was defined as the absence of any movement, excluding breathing and whisker twitches. The total time spent freezing throughout CS presentation is expressed as a percentage of CS duration (10s). Approximately 30% of videos were also scored by a second scorer (R.J.O) and inter-rater reliability was high (r=0.897). Freezing was analyzed with repeated measures ANOVA (within subjects factor = CS number; between subjects factors = sleep group and sex). Extinction data did not meet requirements for sphericity and p values were Greenhouse-Geisser corrected.

Experiment 2 – Spine morphology and density: Rapid Golgi method

Tissue collection and processing

Voles underwent either ELSD or control conditions from P14-P21. As adults (P77-P80) animals were euthanized by an overdose of isoflurane followed by decapitation between 1000h-1200h (ZT3-ZT5) and brains were rapidly removed. Brain tissue was fixed and stained in accordance with manufacturer's instructions (Rapid GolgiStain ™ Kit, FD Neurotechnologies, Inc.). In brief,

brains were bisected into hemispheres, impregnated in Golgi solution and kept in the dark for two weeks, and then kept in a sucrose solution for three days prior to sectioning. Brains were sectioned at 200um (Precisionary Instruments, Greenville, NC), mounted on gelatin coated slides, dehydrated in ethanol series (4 min each: 50% (x1), 75% (x1), 95% (x1), 100% (x4)), cleared with xylenes (three times, 4 min each rinse), and cover slipped with permount. Data presented here were collected from the right hemisphere. Euthanasia was performed between 1000h-1200h (ZT3-ZT5).

Quantitative analyses of spine density and spine morphology

To quantify dendritic spine morphology, Golgi-stained, pyramidal neurons were imaged using a 40x objective (NA = 0.85) on a Leica microscope. Z-stack images (80 μm total on the Z-axis; optical section thickness=2 μm; 41 images per stack; image size, 2,048 x 1,535 pixels (0.1774 X 0.1774 x 2 μm) were acquired using a DFC36 FX camera. One experimenter acquired all images (A.Q.C). Each image stack was extracted using ImageJ software (NIH, Bethesda, MD) and subsequently imported into RECONSTRUCT software [78] for analysis as described in [79]. This method allows for dendrites and spines to be measured in the x, y, and z planes. Pyramidal neurons were imaged from cortical layers 2 and 5 in the PL and IL cortices. The IL and PL were distinguished using the atlas of Franklin and Paxinos (1997) as well as defining cytoarchitecture of Layer 2 in the IL compared to the PL. Only fully impregnated neurons (e.g. no sudden breaks in branches) clearly distinguishable from neighboring neurons were selected for quantification. For each animal, four segments (10-20um) were imaged from apical oblique dendrites from 2-4 pyramidal neurons and values averaged together to create a representative sample from each animal for statistical analysis. To control for sources of variability, segments were selected from each brain to include one secondary and one tertiary dendritic branch from segments both proximal (<80um) and distal (>90um) to the soma wherever staining permitted (4 segments total for each brain). Spine density, length, and width

were quantified, and in this sample, were not significantly different between secondary and tertiary branches or proximal and distal locations and values were averaged together for one representative value for analysis from each animal. All spine quantification was conducted by one experimenter (A.Q.C.) with a small subset confirmed by a second experimenter (R.J.O), both blind to sex and group. The spine density of each segment was calculated by dividing the total number of spines by the length of the corresponding segment. In addition, spine length (L) was measured from the base of the dendritic spine to the tip and spine head width (W) was measured at the widest point. Values met criteria for parametric testing and were compared using ANOVA (between subjects factors = sleep group and sex) for each layer (2 or 5) and P values required for significance were Bonferroni corrected to account for multiple comparisons (alpha = .025).

Experiment 3 – Electron Microscopy

Prairie voles underwent either ELSD (n=4 female; n=6 male) or Control conditions (n=3 female; n=4 male) from P14-P21 and as adults (P70-P110) were deeply anesthetized with ketamine/xylazine cocktail (0.2 mL i.p.) and transcardially perfused with 6mls of phosphate buffer (0.1M, pH 7.3), containing 1000 units/ml of heparin, then followed immediately by 50 mls of EM fixative (2.5% glutaraldehyde/0.5% paraformaldehyde/0.1% picric acid in 0.1 M phosphate buffer, pH 7.3), as previously described[80]. Brains were collected in phosphate buffer, cut in half coronally at the level of the hypothalamus and then further processed in EM fixative in the Biowave (Pelco BioWave, Ted Pella, Inc.) as recently detailed [80]. Brains were collected for EM during the light portion of the light cycle between ZT3-6.

Electron Microscopy (EM) Immunolabeling

Slices containing the prefrontal cortex were processed for EM and imaged as previously described [80, 81]. The tissue was processed using antibodies against the vesicular glutamate

transporter 1 (VGLUT 1: Synaptic Systems, 1:1000, rabbit polyclonal, #135303) and vesicular glutamate transporter 2 (VGLUT2: Synaptic Systems 1:100, rabbit polyclonal, #135403), using our standard immunohistochemistry (IHC) protocol [81-83]. Using tissue samples from each treatment group (3-4 slices/animal), the VGLUT1 and VGLUT2 antibodies were run with all processing carried out in a microwave oven (Pelco BioWave, Ted Pella, Inc.) on the same day. During the IHC processing for electron microscopy Triton X-100 was not used in order to preserve the tissue morphology. Tissue was prepared for electron microscopy as previously reported [80-83].

EM embedding

Tissue was then processed using the same Biowave tissue processor as noted above, with the temperature restricted to less than 60°C for all steps. Tissue was exposed to a solution of 1% osmium tetroxide (OsO_4) (Electron Microscopy Sciences, Hatfield, PA) in 1.5% potassium ferricyanide (Electron Microscopy Sciences, Hatfield, PA) at 100W, with the vacuum cycling for 13 minutes (cycling the magnetron for 3 min on/2 min off/3 min on/2 min off/3 min on). The tissue was then rinsed in deionized Millipore-filtered H_2O (Di H_2O), and the OsO_4 was removed and replaced with Di H_2O, then immediately washed again with fresh Di H_2O in the microwave for two washes (Di H_2O replaced for each wash), 40 sec each, at 150 W, with no vacuum. The tissue was then exposed to a solution of 0.5% uranyl acetate (Electron Microscopy Sciences, Hatfield, PA) in Di H_2O at 100W, cycling vacuum, for 6 min (cycling the magnetron for 2 min on/2 min off/2 min on).

Dehydration and infiltration: An increasing gradient (50%, 75%, 90%, 2×100%) of ethanol in the microwave at 150W was used for 40 sec, with no vacuum at any of the steps. This was then followed by a 40 sec, 150W step exposure to 100% propylene oxide (PO)(Electron Microscopy Sciences, Hatfield, PA), with no vacuum. Tissue was then placed in a 1:1 solution of PO and

EPON/SPURRS resin [84] for 3 min, 200W cycling vacuum, followed by 5×3 min in 100% resin, 200W, cycling vacuum. The tissue slices were then flat embedded between two sheets of ACLAR (Electron Microscopy Sciences, Hatfield, PA) overnight in a 60°C oven in order for the resin to polymerize. The medial prefrontal cortex was micro-dissected out of the embedded tissue and super-glued onto a separate block for each animal. The orientation of the tissue was such that when the tissue was thin sectioned, all six layers of the cortex would be represented in the section to aid in identifying layer 2. The tissue was then thin-sectioned, placed on formvar coated, single-holed slot grids (Electron Microscopy Sciences, Hatfield, PA), followed by post-embed immuno-gold labeling using a primary antibody against glutamate (non-affinity purified, rabbit polyclonal; 1:250, Sigma Chemical Co., St. Louis, MO, #G6642) and a secondary antibody tagged with 12nm gold particles (goat anti-rabbit, 1:50: Jackson ImmunoResearch, West Grove, PA: AB_2338016) was carried out as previously described [80, 81]. The primary glutamate antibody, as previously characterized [80, 85], was diluted in tris buffered saline with triton X-100 (TBST , pH 7.6) in blocking solution [0.5% bovine serum albumin (BSA)] (Electron Microscopy Sciences, Hatfield, PA). Aspartate (1 mM) was added to the glutamate antibody mixture 24 h prior to incubation with the thin-sectioned tissue to prevent any cross-reactivity with aspartate within the tissue. The secondary antibody was goat anti-rabbit IgG (Jackson ImmunoResearch, West Grove, PA; diluted 1:20 in TBST pH 8.2, AB_2338016), tagged with 12 nm gold particles. We previously reported that incubation of the glutamate antibody with 3 mM glutamate resulted in no immuno-gold labeling, showing the specificity of the glutamate labeling [80, 84]. Using a JEM-1400 (JEOL) electron microscope, photographs were randomly taken in DAB labeled areas of Layer 2 (at the leading edge of the tissue section). This layer was easily identifiable within the cortex since this region is just below Layer I, which contains few, if any, neuronal cell bodies.

Morphological analysis

Photographs were taken of DAB labeled terminals (vGlut1, vGlut2) making an asymmetrical synaptic contact onto a spine throughout the neuropil (an area containing the highest numbers of synapses) at a final magnification of ×46,200 by an individual blinded to the experimental groups, using a digital camera (AMT, Danvers, MA). For quantification of glutamate labeling within the nerve terminals, the number of immuno-gold particles located either within, or at least touching the synaptic vesicle membrane (i.e., vesicular pool), the number located outside the synaptic vesicles (i.e., the cytoplasmic pool), and those associated with mitochondria, were counted. The density of glutamate gold labeling within the mitochondria (i.e., metabolic pool) was excluded from the synaptic vesicle/cytoplasmic pool analysis, as previously reported [80, 84]. There are no mitochondria located within dendritic spines. The vesicular and cytoplasmic pools were combined since the cytoplasmic pool is very small (<10%) compared to the vesicular pool [86]. We have reported that nerve terminals making a symmetrical contact contain GABA [86], the precursor for which is glutamate. Therefore, nerve terminals making a symmetrical contact will naturally contain some glutamate immunolabeling and cannot be considered immuno-negative as a way of determining a ratio between glutamatergic and GABAergic terminals [84, 86]. The metabolic pool is also relatively small and thus unlikely to be a major source of variation in labeling density. The density of gold particles/μm^2 of nerve terminal area for the vesicular/cytoplasmic pool was determined for each animal and the mean density for each treatment group calculated. Background labeling was determined within glial cell processes and was found to be about 10 immuno-gold-labeled particles/μm^2 [84, 86]. This was subtracted from the density of presynaptic immuno-gold-labeled glutamate within the vGlut1+ or vGlut2+ nerve terminals. The area of the vGlut1 and vGlut2 labeled terminals was measured along with counting the number of gold particles in the terminal area to determine the density of presynaptic glutamate immuno-gold labeling. The post-synaptic structure was noted as to the type (spine). Photographic analysis was carried out using

ImagePro Premier (MediaCybernetics), and statistical analysis was performed with JMP 11 (SAS). The number of gold particles per terminal, the area, and the density (# gold particles/um^2) was determined for the nerve terminal. Only presynaptic terminals contacting spines were used for analysis.

Independent sample t-tests (two tailed) were conducted on average glutamate density in presynaptic terminals labeled with either vGLUT1 or vGLUT2 and alpha values were Bonferonni corrected to account for multiple comparisons. With this correction, a p-value < 0.025 was required to reject the null hypothesis. Outliers were excluded from analysis and were defined as values greater than 2 standard deviations above or below the mean. Males and females were combined for analysis.

References

1. de Vivo, L., et al., *Ultrastructural evidence for synaptic scaling across the wake/sleep cycle.* Science, 2017. **355**(6324): p. 507-510.
2. Diering, G.H., et al., *Homer1a drives homeostatic scaling-down of excitatory synapses during sleep.* Science, 2017. **355**(6324): p. 511-515.
3. Vyazovskiy, V.V., et al., *Molecular and electrophysiological evidence for net synaptic potentiation in wake and depression in sleep.* Nature neuroscience, 2008. **11**(2): p. 200-208.
4. Li, W., et al., *REM sleep selectively prunes and maintains new synapses in development and learning.* Nature neuroscience, 2017. **20**(3): p. 427-437.
5. Yang, G. and W.B. Gan, *Sleep contributes to dendritic spine formation and elimination in the developing mouse somatosensory cortex.* Developmental neurobiology, 2012. **72**(11): p. 1391-1398.
6. Maret, S., et al., *Sleep and waking modulate spine turnover in the adolescent mouse cortex.* Nature neuroscience, 2011. **14**(11): p. 1418-1420.
7. Roffwarg, H.P., J.N. Muzio, and W.C. Dement, *Ontogenetic development of the human sleep-dream cycle.* Science, 1966.
8. Cui, G.-F., et al., *A Novel Continuously Recording Approach for Unraveling Ontogenetic Development of Sleep-Wake Cycle in Rats.* Frontiers in neurology, 2019. **10**: p. 873.
9. Frank, M.G. and H.C. Heller, *Development of REM and slow wave sleep in the rat.* American Journal of Physiology-Regulatory, Integrative and Comparative Physiology, 1997. **272**(6): p. R1792-R1799.
10. Rensing, N., et al., *Longitudinal analysis of developmental changes in electroencephalography patterns and sleep-wake states of the neonatal mouse.* PloS one, 2018. **13**(11): p. e0207031.

11. Cao, J., et al., *Unraveling why we sleep: Quantitative analysis reveals abrupt transition from neural reorganization to repair in early development.* Science Advances, 2020. **6**(38): p. eaba0398.

12. John, J., L. Ramanathan, and J.M. Siegel, *Rapid changes in glutamate levels in the posterior hypothalamus across sleep-wake states in freely behaving rats.* American Journal of Physiology-Regulatory, Integrative and Comparative Physiology, 2008. **295**(6): p. R2041-R2049.

13. Saper, C.B. and P.M. Fuller, *Wake–sleep circuitry: an overview.* Current opinion in neurobiology, 2017. **44**: p. 186-192.

14. Cruz-Martin, A., M. Crespo, and C. Portera-Cailliau, *Glutamate induces the elongation of early dendritic protrusions via mGluRs in wild type mice, but not in fragile X mice.* PLoS One, 2012. **7**(2): p. e32446.

15. Fremeau Jr, R.T., et al., *The expression of vesicular glutamate transporters defines two classes of excitatory synapse.* Neuron, 2001. **31**(2): p. 247-260.

16. Häusser, M., N. Spruston, and G.J. Stuart, *Diversity and dynamics of dendritic signaling.* Science, 2000. **290**(5492): p. 739-744.

17. Lefebvre, J.L., J.R. Sanes, and J.N. Kay, *Development of dendritic form and function.* Annual review of cell and developmental biology, 2015. **31**: p. 741-777.

18. Hutsler, J.J. and H. Zhang, *Increased dendritic spine densities on cortical projection neurons in autism spectrum disorders.* Brain research, 2010. **1309**: p. 83-94.

19. Purcell, A., et al., *Postmortem brain abnormalities of the glutamate neurotransmitter system in autism.* Neurology, 2001. **57**(9): p. 1618-1628.

20. Horder, J., et al., *Reduced subcortical glutamate/glutamine in adults with autism spectrum disorders: a [1 H] MRS study.* Translational psychiatry, 2013. **3**(7): p. e279-e279.

21. Buckley, A.W., et al., *Rapid eye movement sleep percentage in children with autism compared with children with developmental delay and typical development.* Archives of pediatrics & adolescent medicine, 2010. **164**(11): p. 1032-1037.

22. Nelson, E.E. and A.E. Guyer, *The development of the ventral prefrontal cortex and social flexibility.* Developmental cognitive neuroscience, 2011. **1**(3): p. 233-245.

23. Dalley, J.W., R.N. Cardinal, and T.W. Robbins, *Prefrontal executive and cognitive functions in rodents: neural and neurochemical substrates.* Neuroscience & Biobehavioral Reviews, 2004. **28**(7): p. 771-784.

24. Laurent, V. and R.F. Westbrook, *Inactivation of the infralimbic but not the prelimbic cortex impairs consolidation and retrieval of fear extinction.* Learning & memory, 2009. **16**(9): p. 520-529.

25. Yuen, E.Y., et al., *Acute stress enhances glutamatergic transmission in prefrontal cortex and facilitates working memory.* Proceedings of the National Academy of Sciences, 2009. **106**(33): p. 14075-14079.

26. Milad, M.R. and G.J. Quirk, *Neurons in medial prefrontal cortex signal memory for fear extinction.* Nature, 2002. **420**(6911): p. 70-74.

27. Morgan, M.A., L.M. Romanski, and J.E. LeDoux, *Extinction of emotional learning: contribution of medial prefrontal cortex.* Neuroscience letters, 1993. **163**(1): p. 109-113.

28. Sierra-Mercado, D., N. Padilla-Coreano, and G.J. Quirk, *Dissociable roles of prelimbic and infralimbic cortices, ventral hippocampus, and basolateral amygdala in the expression and extinction of conditioned fear.* Neuropsychopharmacology, 2011. **36**(2): p. 529-538.

29. Memari, A.H., et al., *Cognitive flexibility impairments in children with autism spectrum disorders: links to age, gender and child outcomes.* Research in Developmental Disabilities, 2013. **34**(10): p. 3218-3225.

30. Ozonoff, S., et al., *Performance on Cambridge Neuropsychological Test Automated Battery subtests sensitive to frontal lobe function in people with autistic disorder: evidence from the Collaborative Programs of Excellence in Autism network.* Journal of autism and developmental disorders, 2004. **34**(2): p. 139-150.

31. Jones, C.E., et al., *Early-life sleep disruption increases parvalbumin in primary somatosensory cortex and impairs social bonding in prairie voles.* Science advances, 2019. **5**(1): p. eaav5188.

32. Li, Y., et al., *Effects of chronic sleep fragmentation on wake-active neurons and the hypercapnic arousal response.* Sleep, 2014. **37**(1): p. 51-64.

33. Sinton, C.M., D. Kovakkattu, and R.S. Friese, *Validation of a novel method to interrupt sleep in the mouse.* J Neurosci Methods, 2009. **184**(1): p. 71-8.

34. Jones, C.E., P.T. Wickham, and M.M. Lim, *Early life sleep disruption is a risk factor for increased ethanol drinking after acute footshock stress in prairie voles.* Behavioral Neuroscience, 2020. **134**(5): p. 424.

35. Fremeau Jr, R.T., et al., *VGLUTs define subsets of excitatory neurons and suggest novel roles for glutamate.* Trends in neurosciences, 2004. **27**(2): p. 98-103.

36. Kaneko, T., F. Fujiyama, and H. Hioki, *Immunohistochemical localization of candidates for vesicular glutamate transporters in the rat brain.* Journal of Comparative Neurology, 2002. **444**(1): p. 39-62.

37. Jones, C.E., et al., *Acoustic prepulse inhibition in male and female prairie voles: Implications for models of neuropsychiatric illness.* Behavioural brain research, 2018. **360**: p. 298-302.

38. Kim, J.H., A.S. Hamlin, and R. Richardson, *Fear extinction across development: the involvement of the medial prefrontal cortex as assessed by temporary inactivation and immunohistochemistry.* Journal of Neuroscience, 2009. **29**(35): p. 10802-10808.

39. Loveland, K.A., et al., *Fronto-limbic functioning in children and adolescents with and without autism.* Neuropsychologia, 2008. **46**(1): p. 49-62.

40. South, M., T. Newton, and P.D. Chamberlain, *Delayed reversal learning and association with repetitive behavior in autism spectrum disorders.* Autism Research, 2012. **5**(6): p. 398-406.

41. Top Jr, D.N., et al., *Atypical amygdala response to fear conditioning in autism spectrum disorder.* Biological Psychiatry: Cognitive Neuroscience and Neuroimaging, 2016. **1**(4): p. 308-315.

42. Sala, M., et al., *Pharmacologic rescue of impaired cognitive flexibility, social deficits, increased aggression, and seizure susceptibility in oxytocin receptor null mice: a neurobehavioral model of autism.* Biological psychiatry, 2011. **69**(9): p. 875-882.

43. Banerjee, A., et al., *Abnormal emotional learning in a rat model of autism exposed to valproic acid in utero.* Frontiers in behavioral neuroscience, 2014. **8**: p. 387.

44. Markram, K., et al., *Abnormal fear conditioning and amygdala processing in an animal model of autism.* Neuropsychopharmacology, 2008. **33**(4): p. 901-912.

45. Quirk, G.J., et al., *The role of ventromedial prefrontal cortex in the recovery of extinguished fear.* J Neurosci, 2000. **20**(16): p. 6225-31.

46. Courtin, J., et al., *Prefrontal parvalbumin interneurons shape neuronal activity to drive fear expression.* Nature, 2014. **505**(7481): p. 92-6.

47. Holtmaat, A.J., et al., *Transient and persistent dendritic spines in the neocortex in vivo.* Neuron, 2005. **45**(2): p. 279-291.

48. Condé, F., et al., *Afferent connections of the medial frontal cortex of the rat. A study using retrograde transport of fluorescent dyes. I. Thalamic afferents.* Brain research bulletin, 1990. **24**(3): p. 341-354.

49. Hoover, W.B. and R.P. Vertes, *Anatomical analysis of afferent projections to the medial prefrontal cortex in the rat.* Brain Structure and Function, 2007. **212**(2): p. 149-179.

50. Swanson, L., *A direct projection from Ammon's horn to prefrontal cortex in the rat.* Brain research, 1981. **217**(1): p. 150-154.

51. Van Eden, C., V. Lamme, and H. Uylings, *Heterotopic cortical afferents to the medial prefrontal cortex in the rat. A combined retrograde and anterograde tracer study.* European Journal of Neuroscience, 1992. **4**(1): p. 77-97.

52. Koenderink, M., H. Uylings, and L. Mrzljak, *Postnatal maturation of the layer III pyramidal neurons in the human prefrontal cortex: a quantitative Golgi analysis.* Brain research, 1994. **653**(1-2): p. 173-182.

53. Monique, J.T. and H.B. Uylings, *Postnatal maturation of layer V pyramidal neurons in the human prefrontal cortex. A quantitative Golgi analysis.* Brain research, 1995. **678**(1-2): p. 233-243.

54. Romijn, H.J., M.A. Hofman, and A. Gramsbergen, *At what age is the developing cerebral cortex of the rat comparable to that of the full-term newborn human baby?* Early human development, 1991. **26**(1): p. 61-67.

55. Mattison, H.A., et al., *The role of glutamate in the morphological and physiological development of dendritic spines.* European Journal of Neuroscience, 2014. **39**(11): p. 1761-1770.

56. Wojcik, S.M., et al., *An essential role for vesicular glutamate transporter 1 (VGLUT1) in postnatal development and control of quantal size.* Proceedings of the National Academy of Sciences, 2004. **101**(18): p. 7158-7163.

57. Fremeau, R.T., Jr., et al., *VGLUTs define subsets of excitatory neurons and suggest novel roles for glutamate.* Trends Neurosci, 2004. **27**(2): p. 98-103.

58. Miyazaki, T., et al., *Subtype switching of vesicular glutamate transporters at parallel fibre-Purkinje cell synapses in developing mouse cerebellum.* Eur J Neurosci, 2003. **17**(12): p. 2563-72.

59. Rochefort, N.L. and A. Konnerth, *Dendritic spines: from structure to in vivo function.* EMBO reports, 2012. **13**(8): p. 699-708.

60. Bettendorff, L., et al., *Paradoxical sleep deprivation increases the content of glutamate and glutamine in rat cerebral cortex.* Sleep, 1996. **19**(1): p. 65-71.

61. Cook, S.C. and C.L. Wellman, *Chronic stress alters dendritic morphology in rat medial prefrontal cortex.* Journal of neurobiology, 2004. **60**(2): p. 236-248.

62. Seib, L.M. and C.L. Wellman, *Daily injections alter spine density in rat medial prefrontal cortex.* Neuroscience letters, 2003. **337**(1): p. 29-32.

63. Wellman, C.L., *Dendritic reorganization in pyramidal neurons in medial prefrontal cortex after chronic corticosterone administration.* Journal of neurobiology, 2001. **49**(3): p. 245-253.

64. Brown, S.M., S. Henning, and C.L. Wellman, *Mild, short-term stress alters dendritic morphology in rat medial prefrontal cortex.* Cerebral cortex, 2005. **15**(11): p. 1714-1722.

65. Radley, J., et al., *Chronic behavioral stress induces apical dendritic reorganization in pyramidal neurons of the medial prefrontal cortex.* Neuroscience, 2004. **125**(1): p. 1-6.

66. Radley, J.J., et al., *Repeated stress induces dendritic spine loss in the rat medial prefrontal cortex.* Cerebral cortex, 2006. **16**(3): p. 313-320.

67. Kolb, B., et al., *Experience and the developing prefrontal cortex.* Proceedings of the National Academy of Sciences, 2012. **109**(Supplement 2): p. 17186-17193.

68. Kim, Y., et al., *Mapping social behavior-induced brain activation at cellular resolution in the mouse.* Cell reports, 2015. **10**(2): p. 292-305.

69. Yizhar, O., et al., *Neocortical excitation/inhibition balance in information processing and social dysfunction.* Nature, 2011. **477**(7363): p. 171-178.

70. Murugan, M., et al., *Combined social and spatial coding in a descending projection from the prefrontal cortex.* Cell, 2017. **171**(7): p. 1663-1677. e16.

71. Selimbeyoglu, A., et al., *Modulation of prefrontal cortex excitation/inhibition balance rescues social behavior in CNTNAP2-deficient mice.* Science translational medicine, 2017. **9**(401): p. eaah6733.

72. Hrabovszky, E. and Z. Liposits, *Novel aspects of glutamatergic signalling in the neuroendocrine system.* Journal of neuroendocrinology, 2008. **20**(6): p. 743-751.

73. Young, L.J., et al., *Cellular mechanisms of social attachment.* Hormones and behavior, 2001. **40**(2): p. 133-138.

74. Tan, Y., et al., *Oxytocin receptors are expressed by glutamatergic prefrontal cortical neurons that selectively modulate social recognition.* Journal of Neuroscience, 2019. **39**(17): p. 3249-3263.

75. Hammock, E. and P. Levitt, *Oxytocin receptor ligand binding in embryonic tissue and postnatal brain development of the C57BL/6J mouse.* Frontiers in behavioral neuroscience, 2013. **7**: p. 195.

76. MacDuffie, K.E., et al., *Sleep onset problems and subcortical development in infants later diagnosed with autism spectrum disorder.* American Journal of Psychiatry, 2020. **177**(6): p. 518-525.

77. Simola, P., et al., *Psychosocial and somatic outcomes of sleep problems in children: A 4-year follow-up study.* Child: care, health and development, 2014. **40**(1): p. 60-67.

78. Fiala, J.C., *Reconstruct: a free editor for serial section microscopy.* Journal of microscopy, 2005. **218**(1): p. 52-61.

79. Risher, W.C., et al., *Rapid Golgi analysis method for efficient and unbiased classification of dendritic spines.* PLoS One, 2014. **9**(9): p. e107591.

80. Moore, C., et al., *Differential ultrastructural alterations in the Vglut2 glutamatergic input to the substantia nigra pars compacta/pars reticulata following nigrostriatal dopamine loss in a progressive mouse model of Parkinson's disease.* European Journal of Neuroscience, 2020.

81. Parievsky, A., et al., *Differential electrophysiological and morphological alterations of thalamostriatal and corticostriatal projections in the R6/2 mouse model of Huntington's disease.* Neurobiol Dis, 2017. **108**: p. 29-44.

82. Spinelli, K.J., et al., *Presynaptic alpha-synuclein aggregation in a mouse model of Parkinson's disease.* J Neurosci, 2014. **34**(6): p. 2037-50.

83. Walker, R.H., et al., *Effects of subthalamic nucleus lesions and stimulation upon corticostriatal afferents in the 6-hydroxydopamine-lesioned rat.* PLoS One, 2012. **7**(3): p. e32919.

84. Meshul, C.K., et al., *Haloperidol-induced morphological changes in striatum are associated with glutamate synapses.* Brain Res, 1994. **648**(2): p. 181-95.

85. Phend, K.D., R.J. Weinberg, and A. Rustioni, *Techniques to optimize post-embedding single and double staining for amino acid neurotransmitters.* J Histochem Cytochem, 1992. **40**(7): p. 1011-20.

86. Meshul, C.K., et al., *Time-dependent changes in striatal glutamate synapses following a 6-hydroxydopamine lesion.* Neuroscience, 1999. **88**(1): p. 1-16.